Band simulation based pan-sharpening algorithm by linear regression for IKONOS imagery

WANG Zhong-wu[1,2], **ZHAO Zhong-ming**[2], **LIU Shun-xi**[1]

1. *China Land Surveying & Planning Institute, Beijing* 100035, *China*;
2. *Institute of Remote Sensing Applications, Chinese Academy of Sciences, Beijing* 100101, *China*

Abstract: In the general fusion framework of optical remote sensing image fusion, the extraction of spatial detail information is one of the two key aspects for the fusion quality. This paper discusses the possibility of constructing the low resolution panchromatic image based on band simulation using linear regression. Firstly, a linear regression equation between panchromatic and multispectral images was modeled, followed by setting weight metric from the corresponding high frequency component of the panchromatic image; then, low resolution panchromatic image was simulated by the regression parameters got in the first step and the spatial detail was extracted; finally, the pan-sharpening procedure was implemented with the spatial detail on IKONOS multispectral and panchromatic imagery. Compared with the method of achieving low resolution panchromatic image based on spectral response function, the proposed method can perform as good as, and sometimes even better than that according to four experiments. Also, the proposal shows its superiority over fast intensity-hue-saturation method.

Key words: pan-sharpening, spatial detail information, band simulation

CLC number: TP751.1 **Document code:** A

Citation format: Wang Z W, Zhao Z M and Liu S X. 2010. Band simulation based pan-sharpening algorithm by linear regression for IKONOS imagery. *Journal of Remote Sensing*. 14(1): 043—054

1 INTRODUCTION

Limited by incoming radiation energy and data volume, most sensors collect high resolution panchromatic (PAN) and low resolution multispectral (MS) images together, instead of high-resolution MS images directly (Zhang, 2004). It is clear that the most effective solution of providing high resolution MS is to develop effective image fusion techniques. Various image fusion methods have been proposed, however, for image fusion of very high resolution data (e.g. IKONOS and QuickBird), the fusion quality is always determined by the extent of spectral information preservation, which dwarfs quite a few traditional methods (Tu *et al.*, 2004).

The studies on general framework of image fusion revealed that spatial detail and its injecting manner were the main reasons for color distortion in image fusion. For the first one, the spectral response function (SRF) method had been paid more attention. Tu *et al.* (2004) added near-inferred band into the procedure of constructing low resolution PAN (LRP) to increase the correlation between PAN and LRP, and to reduce the color distortion. María (2006) adopted SRF in obtaining the weight parameters while simulating LRP from MS. Dou *et al.* (2007) constructed HRP and LRP considering SRF of IKONOS, then calculated the difference and regarded the delta image between the difference image and its mathematical expectation as spatial information.

However, it is hard to get weighting parameters for images collected by sensors without SRF measured in the same situation. So a general method to achieve the weighting parameters should be studied. Shettigara (1989) proposed the linear transformation method, but he did not consider the effects of high frequency pixels. In this paper, we mainly aimed at the probability of simulating LRP by linear regression in the fusion of IKONOS MS+PAN imageries.

2 GENERAL FRAMEWORK OF IMAGE FUSION

The general framework of image fusion is described by Dou (2006) in Eq. (1).

$$\mathrm{HRM} = \mathrm{LRM} + W\delta \tag{1}$$

where HRM is the fusion result; LRM is the resampled image of MS having the same size with PAN, W is the injecting parameter (also called modulation coefficient), and δ is spatial detail of redundant information. Traditionally, δ is calculated as δ = HRP–LRP (Wang, 2005), while HRP is high resolution PAN, the original PAN quite often. In this case, the quality of

Received: 2008-10-14; **Accepted**: 2009-05-12

Foundation: Key Projects in the National Science & Technology Pillar Program (No. 2008BAJ11B06), National High Technology Research and Development Program of China (863 Program) (No. 2007AA1202031).

First author biography: WANG Zhong-wu (1983—), male, Ph.D, majoring in land remote sensing, optical remote sensing image processing, having published 5 papers. E-mail: ripewzw0514@126.com

image fusion is determined by LRP and W.

3 DATASETS AND METHODS

The comparisons were carried out on the proposed method and the SRF method, expressed at (Space Imaging, 2008). To get the reference of quality assessment, Wald's strategy was adopted. Original PAN and MS images were spatially degraded down to a lower resolution in order to compare the fused product to the only genuine references, formed by MS original set. The workflow could be described as Fig. 1, of which the number in brackets indicates the image size.

3.1 Experiment datasets

Two scenes of IKONOS were used in this paper, and totally four MS+PAN datasets were experimented. Spatial resolution of PAN and MS are 1 m and 4m respectively. The first scene locates in Jixian, Tianjin, China, collected on March 21, 2001. The image shows a natural area, including bare rocks on mountains, low-density residential areas, terrace and alleys among mountains, while the whole image size of PAN is 7288×6780 pixels. A subset of 6000×6000 pixels in PAN and the corresponding region in MS were the first dataset (Fig. 2(a), Fig. 2 (b)). And, two small fragment of 400×400 pixels in PAN and

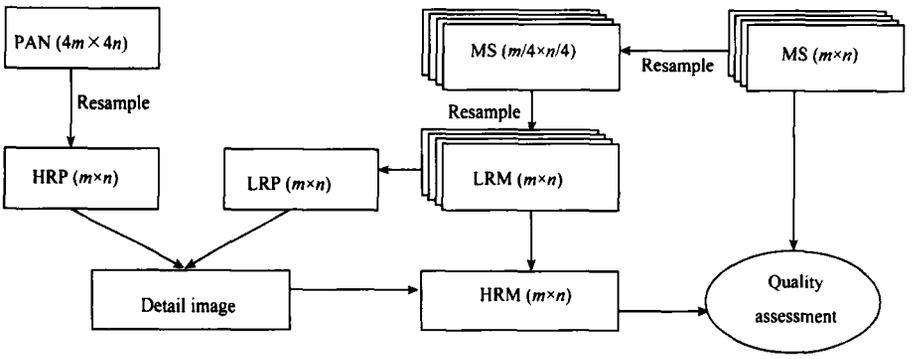

Fig. 1 Workflow

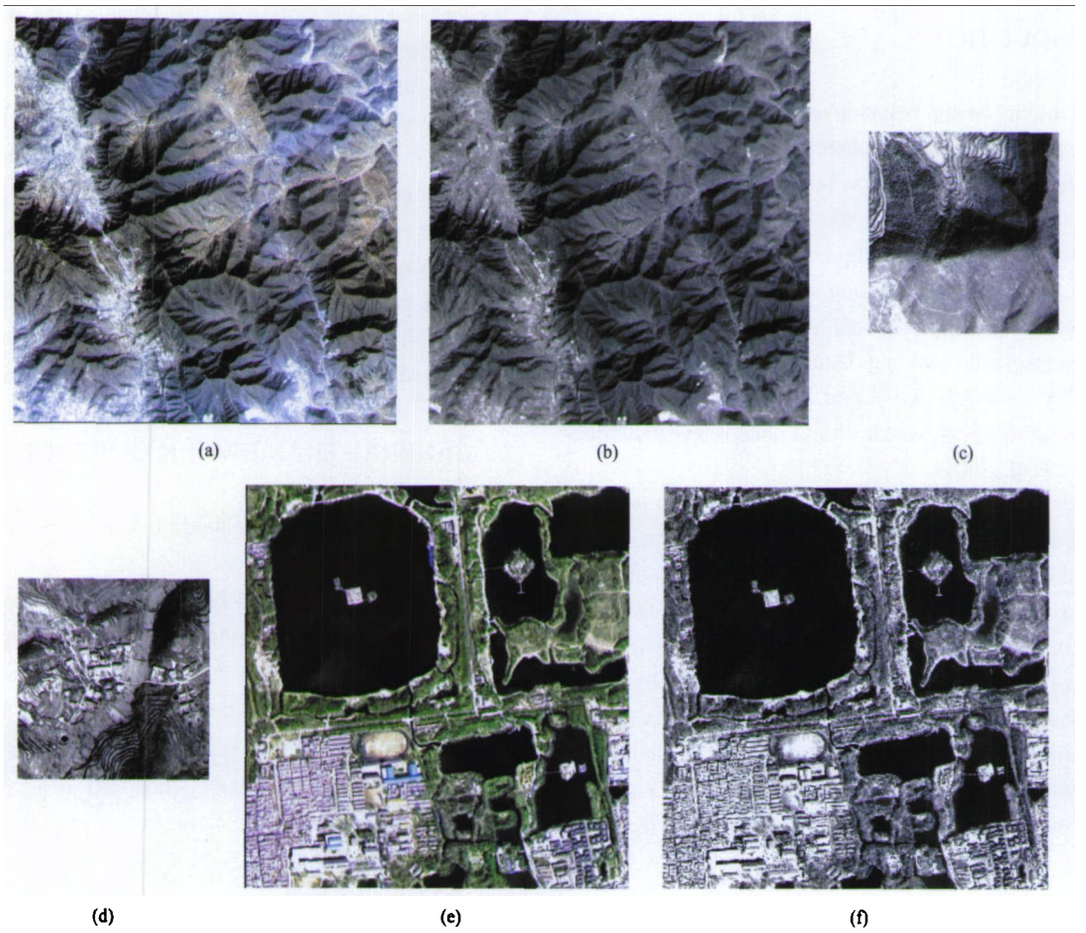

Fig. 2 Source MS and PAN images

(a) MS of dataset 1; (b) PAN of dataset 1; (c) PAN of dataset 2; (d) PAN of dataset 3; (e) MS of dataset 4; (f) PAN of dataset 4

the corresponding region in MS were cropped to be the second and the third datasets, aiming at testing the usage of the proposed method on images coving various ground objects, of whom the first one got few high frequency (PAN is as shown in Fig. 2(c)) and the other one included much more high frequency (PAN is as shown in Fig.2(d)). The second scene lies in Beijing, China, collected on July 18, 2007. Ground objects are mainly small lakes, grass and trees, roads and buildings in urban city. Also a subset of 1200×1200 pixels in PAN and the corresponding region in MS were used as the fourth dataset (Fig. 2(e), (f)).

3.2 The new method

The purpose of this paper is to identify the probability of constructing LRP by linear regression from LMS. Since there is no recommended value of injecting parameter W, which is independent of δ and has non business with simulating LRP, we set W to be {1,1,1,1}, the same as traditional intensity-hue-saturation (IHS) fusion method.

The fusion model of simulating LRP by SRF method is linear regression equation without constant between LRP and LRM.

$$\mathrm{LRP}_{(i,j)} = \sum_{k=1}^{4} c_k \mathrm{LRM}_{k(i,j)} \tag{2}$$

where k is the band number of LMS, (i, j) is the i^{th} row and the j^{th} volume pixel, c_k is the weighting parameter, calculated by SRF (Xavier *et al.*, 2005).

As is known to us, SRF method only considers nominal spectral responses in laboratory. However, atmospheric scattering in on-orbit working conditions, mixed pixels, spectral range of sensors *etc.*, can significantly affect the response of spectral (Space Imaging, 2008). Therefore, it is more reasonable to calculate weight parameter from the processed images. It is noticeable that, detail information such as edges and noise could not be captured by sensors with lower resolution, so high frequency pixels does not satisfy the linear regression equation (Eq. (2)), and should be regarded as outliers. According to the theory, the implementation steps could be summarized as: (1) Re-sample MS to the same size with PAN to be LRM and set PAN to be LRP in Eq. (2). (2) Get HP image by high-pass filtering on PAN and set weighting coefficient matrix P. (3) Build linear regression equation and resolve the weight parameters (Eq. (3)).

$$\mathrm{LRP}_{(i,j)} = \sum_{k=1}^{4} c'_k \mathrm{LRM}_{k(i,j)}, P = \frac{\max(\mathrm{HP}) - \mathrm{HP}}{\max(\mathrm{HP}) - \min(\mathrm{HP})} \tag{3}$$

Generally, Modular Transfer Function (MTF) can compensate the differences on spatial information among images of different levels from the same satellite and the same time. As MTF is always unknown (Garzelli *et al.*, 2008), high-pass filtering is an available options. Compared with the frequency domain high-pass filter, the spatial domain high-pass filter has the advantage of simpler calculation and faster processing speed. For the spatial domain high-pass filter, two famous filters are gradient high-pass filter and Laplacian high-pass filter, while the former can extract gray mutations in a given direction and the latter can detect gray changes of all directions. To our problem, the effects of all high frequency must be kicked out. Therefore, Laplacian high-pass filter is a good choice for reducing the effects of high frequency in simulating LRP. Furthermore, the spatial resolution ratio between MS and Pan (r) indicates the energy of a ground region entering into the sensor in image formation, and it is reasonable to involve r into setting the kernel size of high-pass filter. In the case, a recommended scheme is to consider $(2r+1)\times(2r+1)$ pixels of a given neighborhood, while r is r=4m/1m=4 and the kernel size is 9×9 for IKONOS image, and the high-pass filter used in our method is Eq. (4):

$$\begin{bmatrix} -1 & -1 & -1 & -1 & -1 & -1 & -1 & -1 & -1 \\ -1 & -1 & -1 & -1 & -1 & -1 & -1 & -1 & -1 \\ -1 & -1 & -1 & -1 & -1 & -1 & -1 & -1 & -1 \\ -1 & -1 & -1 & -1 & -1 & -1 & -1 & -1 & -1 \\ -1 & -1 & -1 & -1 & 80 & -1 & -1 & -1 & -1 \\ -1 & -1 & -1 & -1 & -1 & -1 & -1 & -1 & -1 \\ -1 & -1 & -1 & -1 & -1 & -1 & -1 & -1 & -1 \\ -1 & -1 & -1 & -1 & -1 & -1 & -1 & -1 & -1 \\ -1 & -1 & -1 & -1 & -1 & -1 & -1 & -1 & -1 \end{bmatrix} \tag{4}$$

Then, Eq. (3) can be transformed to Eq. (5) as follows,

$$\mathrm{LRP} = C' \times \mathrm{LRM},\ C' = (\mathrm{LRM}^{\mathrm{T}} \times P \times \mathrm{LRM})^{-1} \mathrm{LRM}^{\mathrm{T}} \times P \times \mathrm{LRP} \tag{5}$$

where C' is regression coefficient, also called weighting parameter; P, a diagonal matrix which can kick out the outliers caused by edge pixels and improve simulating precise, is weight coefficient matrix of least square method, other parameters are the same with Eq. (2). In another fact, as remote sensing imageries are huge generally, pixels of a given number randomly selected could be used as observation while solving the regression problem.

3.3 Quality assessment

Q_4 (Alparone *et al.*, 2004) can measure color distortion between the fusion result and the reference from three aspects, which are brightness, contrast and correlative coefficient. The formula is Eq. (6).

$$Q_4 = \frac{1}{|\omega|} \sum_{w \in \omega} Q_4(z_1, z_2 \mid w),$$

$$Q_4(z_1, z_2) = \frac{4 \left| \sigma_{z_1 z_2} \right| \cdot \left| \bar{z}_1 \right| \cdot \left| \bar{z}_2 \right|}{(\sigma_{z_1}^2 + \sigma_{z_2}^2)(\left| \bar{z}_1 \right|^2 + \left| \bar{z}_2 \right|^2)} \tag{6}$$

where, z_1, z_2 are the quaternions formed by the gray values of all bands in HRM and the reference individually. The higher Q_4 is, the more similar the fusion result is with the reference, the better the fusion performs, and vice versa. Although Q_4 depends on the window size, it is easy to decide the performance order of fusion methods at a fixed windows size (16×16 pixels is used in this paper), and the conclusion is independent of windows size (Alparone *et al.*, 2004).

4 EXPERIMENTS AND ANALYSIS

LRP simulated by SRF method and linear regression method are both integrated into the fusion procedure and compared with each other. In the linear regression method, 2000 pixels are randomly selected to solving weighting parameters in the first and fourth datasets considering its mass pixels. For the second and third datasets, three ways are tested, e.g., all pixels, 1000 randomly selected pixels and 2000 randomly selected pixels. Fig. 3 shows HRP and LRP of four datasets, while LRP_SRF is LRP simulated by SRF method, and that LRP_LSAll, LRP_LS1000 and LRP_LS2000 are LRP simulated by linear regression with all pixels, 1000 randomly selected pixels and 2000 randomly selected pixels, respectively.

Comparing LRP with HRP in Fig. 3, for the first dataset, resident and road seem to be brighter, while terrace, rock and mountain follows, and shadows of mountain is the darkest. For the second dataset, the order according to the brightness from high to low is terrace, road, rock and shadow. For the third dataset, the order according to the brightness is resident, terrace, rock and shadow. For the fourth dataset, roads and building are brighter; vegetable is a litter darker; and lake is the darkest. In a whole, for all the four datasets, HRP and LRP have a higher similarity, and it is hard to tell the difference between LRP simulated by SRF method and linear regression method.

Fast intensity-hue-saturation (FastIHS) (Tu, 2004) sets the average image of four bands to be LRP, while the injecting parameter W is the same with our method. The superiority could be easily reported on the comparison. Fig. 4 lists the fusion results of FastIHS and the proposed method on the first and fourth datasets, while HRM_FIHS is that of FastIHS and that HRM_SRF and HRM_LS2000 are results based on LRP_SRF and LRP_LS2000. For the first dataset, all methods get high resolution multispectral image having almost the same

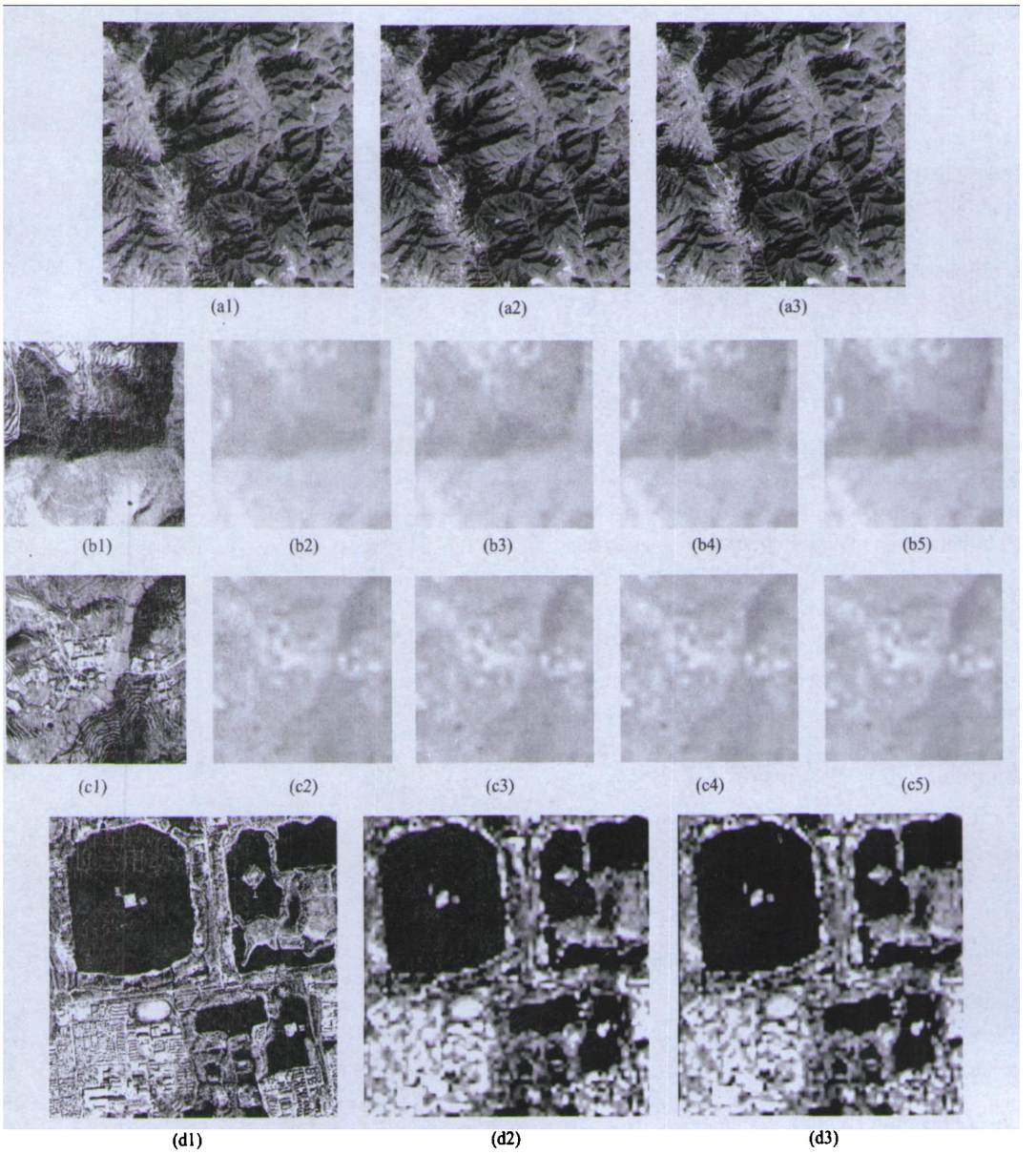

Fig. 3 LRP simulation of four datasets

(a1) HRP; (a2) LRP_SRF; (a3) LRP_LS2000; (b1) HRP; (b2) LRP_SRF; (b3) LRP_LSAll; (b4) LRP_LS1000; (b5) LRP_LS2000; (c1) HRP; (c2) LRP_SRF; (c3) LRP_LSAll; (c4) LRP_LS1000; (c5) LRP_LS2000; (d1) HRP; (d2) LRP_SRF; (d3) LRP_LS2000

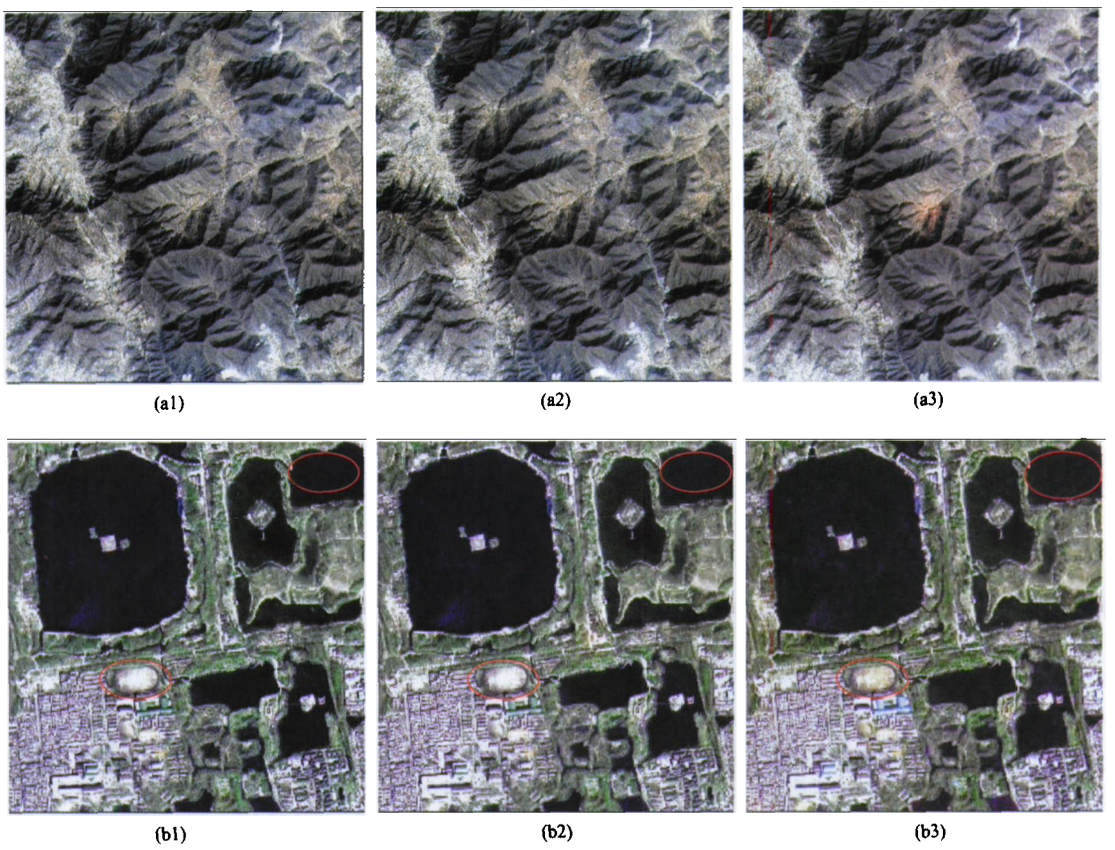

Fig. 4 Fusion results based on LRP_LS2000 and LRP_SRF of two datasets
(a1) HRM_FIHS; (a2) HRM _SRF; (a3) HRM_ LS2000; (b1) HRM_FIHS; (b2) HRM _SRF; (b3) HRM_ LS2000

color with the original MS, so as to the tiny difference could not be found at a rough glance. For the fourth dataset, all methods get high resolution multispectral image, too. But, for the lake highlighted by the red ellipse in the up-right, HRM_LS2000 is much purpler and more similar to the reference, while the other two is bluer. Furthermore, for the playground also highlighted by the red ellipse in the mid, HRM_LS2000 performs better either, appearing much more yellow than the others. All the evidence indicates the superiority of HRM_LS2000 in retaining spectral information. Since the injecting parameters of these methods are the same, it can be safely to conclude that the quality improvement is due to the method of simulating LRP.

Both qualitative and quantitative assessments are performed. Table 1 reports the weighting parameters, correlation coefficient between HRP and LRP of different methods on the four datasets, and also the Q_4 quality indices. It can be observed that:

Table 1 Weight parameters, correlation coefficient between HRP and LRP as well as Q_4 of different methods

Dataset	Simulating method	Weighting parameters	CC with HRP	Q_4
1	LRP_SRF	0.1965, 0.2350, 0.2367, 0.2454	0.8867	0.8294
	LRP_LS2000	0.1042, 0.1484, 0.3408, 0.3408	0.8872	**0.8303**
	FastIHS	0.2500, 0.2500, 0.2500, 0.2500	0.8866	0.8284
2	LRP_SRF	0.1965, 0.2350, 0.2367, 0.2454	0.8541	0.7921
	LRP_LSAll	0.0241, 0.2817, 0.3236, 0.2882	0.8543	0.7923
	LRP_LS1000	0.0392, 0.2731, 0.2973, 0.3061	0.8543	**0.7926**
	LRP_LS2000	0.0391, 0.2509, 0.3208, 0.3103	0.8543	0.7923
3	LRP_SRF	0.1965, 0.2350, 0.2367, 0.2454	0.6668	**0.8371**
	LRP_LSAll	0.2045, 0.2836, 0.2344, 0.1936	0.6674	0.8366
	LRP_LS1000	0.2909, 0.1200, 0.2906, 0.2290	0.6667	0.8349
	LRP_LS2000	0.2173, 0.3272, 0.0953, 0.2684	0.6665	0.8360
4	LRP_SRF	0.1965, 0.2350, 0.2367, 0.2454	0.7407	0.7987
	LRP_LS2000	0.0500, 0.3695, 0.0500, 0.5095	0.7507	**0.8078**
	FastIHS	0.2500, 0.2500, 0.2500, 0.2500	0.7381	0.7976

(1) From correlation coefficient between HRP and LRP, our method could simulated LRP on all datasets efficiently, with tiny differences to SRF method.

(2) From the Q_4 indices, fusion result based on LRP by linear regression performed comparable or better than SRF method.

(3) The weighting parameters by LRP_SRF and LRP_LS are not the same. The reason could be: if high correlation occurs between neighborhood bands of multispectral images, the design matrix of normal equation has a certain degree of singularity and the conditions of coefficient matrix are huge, so that the weighting parameters is unstable while solving the least square problem (Wang, 2004).

(4) The number of randomly selected pixels causes distinctive performances, but not significantly.

5 CONCLUSIONS

Extracting spatial detail information is crucial for the fusion of MS+PAN imageries. This paper identifies the probability of constructing low resolution panchromatic imagery by linear regression from low resolution multispectral image. Validating experiments were carried out on four IKONOS multispectral and panchromatic datasets, results show that the proposed method can perform as good as, and sometimes even better than that. Also, the proposal shows its superiority over fast intensity-hue-saturation fusion method, too. It is noticeable that the new method does not need any priori knowledge and leads to a better practicable potential. Future work will be carried out on optimizing linear regression model, reducing singularity in the design matrix of normal equation, and other types of remote sensing images.

REFERENCES

Alparone L, Baronti S, Garzelli A and Nencini F. 2004. A global quality measurement of pan-sharpened multispectral imagery. *IEEE Transactions on Geoscience and Remote Sensing Letters*, **1**(4): 313—317

Dou W, Chen Y H, Li X B and Sui D Z. 2007. A general framework for component substitution image fusion: an implementation using the fast image fusion method. *Computers & Geosciences*, **33**: 219—228

Dou W. 2006. Research on the Universal Theoretical Framework for Multi-source Remotely Sensed Data. Beijing: Beijing Normal University

Garzelli A, Nencini F and Capobianco L. 2008. Optimal MMSE pan sharpening of very high resolution multispectral images. *IEEE Transactions on Geoscience and Remote Sensing*, **46**(1): 228—236

María G A, Xavier O, Octavi F and Jesús A M. 2006. A low computational-cost method to fuse IKONOS images using the spectral response function of its sensors. *IEEE Transactions on Geoscience and Remote Sensing*, **44**(6): 1683—1691

Shettigara K V. 1989. A linear transformation technique for spatial enhancement of multispectral images using a higher resolution data set. IGARSS'89, **4**: 2615—2618

Space Imaging. 2008. IKONOS 2 Relative Spectral Response [EB/OL]. http://www.geoeye.com/CorpSite/resource/white papers.aspx. (2 Feb, 2009)

Tu T M, Huang P S, Hung C L and Chang C P. 2004. A fast intensity-hue-saturation fusion technique with spectral adjustment for IKONOS imagery. *IEEE Geoscience and Remote Sensing Letters*, **1**(4): 309—312

Wald L, Ranchln T and Mangolini M. 1997. Fusion of satellite images of different spatial resolutions: assessing the quality of resulting images. *Photogrammetric Engineering & Remote Sensing*, **6**: 691—699

Wang Z J, Ziou D, Armenakis C, Li D R and Li Q Q. 2005. A comparative analysis of image fusion methods. *IEEE Transactions on Geoscience and Remote Sensing*, **43**(6): 1391—1402

Wang Z J. 2004. Determining the ridge parameter in a ridge estimation using L-curve method. *Geomatics and Information Science of Wunan University*, **29**(3): 235—238

Xavier O, María G A, Octavi F and Jorge N. 2005. Introduction of sensor spectral response into image fusion methods: application to wavelet-based methods. *IEEE Transactions on Geoscience and Remote Sensing*, **43**(10): 2376—2385

Zhang Y. 2004. Understanding image fusion. *Photogrammetric Engineering & Remote Sensing*, **6**: 657—661

IKONOS 图像的线性回归波段拟合融合方法

王忠武[1,2], 赵忠明[2], 刘顺喜[1]

1. 中国土地勘测规划院, 北京 100035;
2. 中国科学院 遥感应用研究所, 北京 100101

摘 要: 讨论基于线性回归波段拟合的空间细节信息提取方法的可行性。首先通过全色与多光谱图像构造线性回归方程, 根据全色图像的高频成分设置最小二乘求解的权系数, 然后利用回归系数构造低分辨率的全色图像, 提取空间细节信息, 最后将空间细节注入多光谱图像中进行融合。通过 IKONOS 全色和多光谱图像的融合实验, 比较了本文方法与基于光谱响应函数的方法, 结果表明: 采用本文方法提取的空间细节信息进行融合, 能达到甚至超过基于光谱响应函数方法的融合质量; 相对于与 FastIHS 融合方法, 本文方法的融合质量也有较大的提高。

关键词: 融合, 空间细节信息, 波段拟合

中图分类号: TP751.1 **文献标识码:** A

引用格式: 王忠武, 赵忠明, 刘顺喜. 2010. IKONOS 图像的线性回归波段拟合融合方法. 遥感学报, 14(1): 043—054
Wang Z W, Zhao Z M and Liu S X. 2010. Band simulation based pan-sharpening algorithm by linear regression for IKONOS imagery. *Journal of Remote Sensing*. 14(1): 043—054

1 引 言

受到技术的限制, 大多数的卫星平台同时搭载多光谱(multispectral, MS)波段传感器和全色(panchromatic, PAN)波段传感器(Zhang, 2004)。为了便于遥感图像的应用, 采用融合的手段获得具有丰富光谱信息和高空间分辨率的图像。过去几十年, 大量的融合方法被提出, 然而, 对于超高分辨率的卫星图像(IKONOS, QuickBird 等)的融合, 这些方法引起显著的光谱变形(Tu, 2004)。

像元级融合统一理论框架(Dou, 2006)的提出, 使人们找到了光谱变形的根源, 即空间细节信息提取方法及其注入方式。对于空间细节信息的提取, 基于光谱响应函数(spectral response function, SRF)的方法得到了较大关注。Tu 等(2004)计算低分辨率全色图像(low resolution PAN, LRP) 时加入近红外波段, 使之与高分辨率全色图像(high resolution PAN, HRP)的相关性增大, 降低了 IKONOS 图像融合结果的光谱变形; María 等(2006)利用 IKONOS 的 SRF, 计算各多光谱波段线性拟合 LRP 时的系数; Dou 等(2007)根据 IKONOS 的 SRF 构建出高分辨率和低分辨率的亮度图像, 然后将两者之差与其均值图像的差值作为细节信息。

然而, 对于没有在同一环境下测定光谱响应函数的传感器获取的图像, 无法计算出构造 LRP 的线性加权系数, 有必要研究通用的构造 LRP 的方法。Shettigara(1989)提出了线性变换构造 LRP 的方法, 然而没有考虑不同分辨率图像中高频信息的影响。本文对 IKONOS 图像进行融合实验, 讨论通过线性回归的方式获取 LRP 的可行性。

2 像元级融合统一理论框架

Dou(2006)将数学推导和物理假设分离, 提出了像元级融合统一理论框架:

$$\mathrm{HRM} = \mathrm{LRM} + W\delta \tag{1}$$

式中, HRM 表示融合后的高分辨率多光谱图像; LRM 表示重采样的低分辨率多光谱图像; W 表示空间细节注入方式; δ 表示空间细节信息, 目前常用的空间细节信息计算方法为δ = HRP−LRP (Wang,

收稿日期: 2008-10-14; **修订日期:** 2009-05-12

基金项目: 国家科技支撑计划(编号: 2008BAJ11B06)和国家高技术研究发展计划("863"计划)(编号: 2007AA1202031)。

第一作者简介: 王忠武(1983—), 男, 博士, 2009 年毕业于中国科学院遥感应用研究所, 发表论文 5 篇, 目前主要从事土地遥感和光学遥感图像处理的研究工作。E-mail: ripewzw0514@126.com。

2005), HRP 表示高分辨率的全色图像, LRP 表示低分辨率的全色图像。通常情况下, HRP 为融合输入全色图像, 所以影响融合质量的实际因素为: W 和 LRP。

3 实验数据与方法

IKONOS 全色与多光谱传感器的 SRF 已经发布(Space Imaging, 2008), 拟将本文方法与 SRF 的方法进行比较。为了获得融合质量评价的参考图像, 采用了 Wald(1997)的策略, 将原始多光谱图像作为参考图像, 对全色图像和多光谱图像进行降采样, 使其长度和宽度分别为原图像的 1/4, 然后对采样后的图像进行融合, 并将融合结果与原始多光谱图像进行比较。总体流程图如图 1, 括号内的值表示图像的大小。

3.1 实验数据

本文使用两组 IKONOS 全色与多光谱数据进行 4 组融合实验, 第 1 组数据实验区位于天津市蓟县, 区域内山脉较多, 地物类型有大量的裸露岩石、分布较分散的居民区、梯田以及连接居民区的道路等, 图像获取时间为 2001-03-12, 全色和多光谱图像空间分辨率分别为 1m 和 4m, 全色图像大小为 7288 × 6780 像元。从全色图像上截取 6000 × 6000 像元的区域图像, 在多光谱图像上截取相应的区域图像, 作为第 1 组融合实验数据, 如图 2(a)、2(b)。同时, 为了测试本文方法在不同地物类型中的实用性, 从全色图像上截取 2 个 400 × 400 像元的区域图像, 从多光谱图像上截取相应的区域, 分别作为第 2、3 组融合实验数据, 其中, 第 2 组融合实验数据中的地物为大量的裸露岩石、少量梯田, 整体上图像边缘细节信息较少, 全色图像如图 2(c); 第 3 组融合实验数据中的地物为大量的居民区、少量梯田以及山上的岩石, 整体上图像边缘细节信息较多, 全色图像如图 2(d)。

第 2 组数据实验区位于北京市海淀区, 地物类型主要有房屋、街区道路、湖泊和植被, 获取时间为 2007-07-18, 从全色图像中截取大小为 1200 × 1200 像元的区域, 以及多光谱图像上相应区域作为第 4 组融合实验数据, 如图 2(e)、2(f)。

3.2 融合方法

本文的目的在于研究基于线性回归构造 LRP 的可能性, 由于空间细节的注入方式 W 还没有形成统一的定论, 而且在式(1)中, W 表现为 δ 注入 LRM 的量的多少, 与 δ 相互独立, 不会对 LRP 的拟合产生影响, 故本文中, 将 W 设置为{1,1,1,1}, 与传统 IHS 融合方法的 W 相同(Wang, 2005), 便于在相同的 W 下与 IHS 方法进行横向比较。

基于 SRF 构造 LRP 的模型为不含常数项的多元一次线性回归模型, 表示为:

$$\mathrm{LRP}_{(i,j)} = \sum_{k=1}^{4} c_k \mathrm{LRM}_{k(i,j)} \tag{2}$$

式中: k 为多光谱图像的波段号; (i, j) 为图像的第 i 行第 j 列; c_k 为线性加权系数, 由 SRF 计算得到(Xavier 等, 2005)。

基于线性回归波段拟合构造 LRP 的方法认为: 由于 SRF 是在指定环境下测定, 在遥感图像的成像过程中, 受到很多不确定的因素的影响, 例如大气散射、混合像元、传感器波段光谱范围等, 使实际环境与理想环境存在差距, 导致获取加权系数并不能最优; 根据当前图像拟合加权系数更符合实际情况; 此外, 边缘细节像元无法通过简单的多元一次回归方程拟合, 方程求解时应将其作为观测值中粗差进行处理。该方法的步骤为: 首先将输入多光谱图像重采样至输入全色图像的大小, 并作为线性回归方程中的 LRM, 将输入全色图像作为回归方程中的 LRP; 然后对输入全色图像进行高通滤波, 并采用高频细节图像 HP 设置最小二乘求解回归系数时的权值; 最后构造线性回归方程, 并求解回归系数。

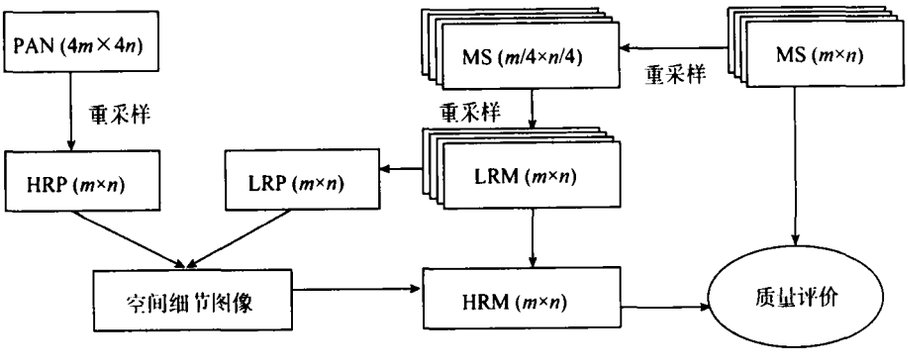

图 1 本文方法的流程图

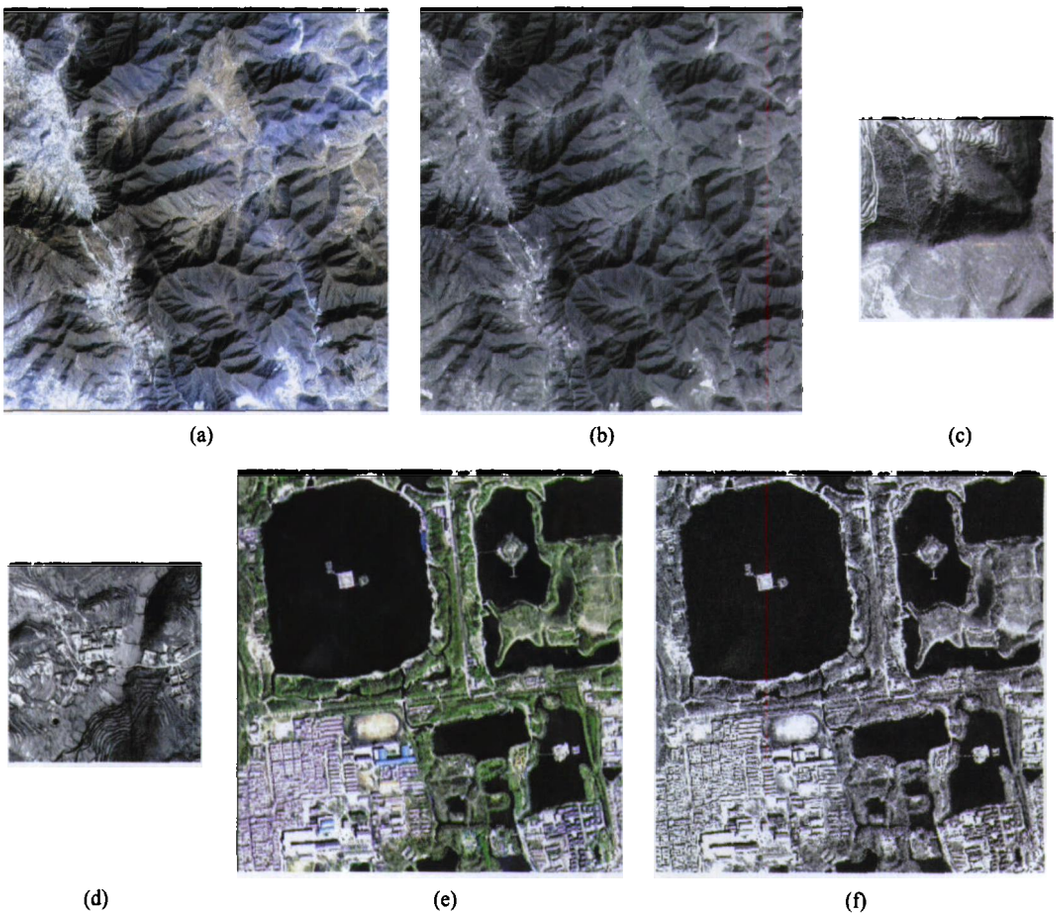

(a) (b) (c) (d) (e) (f)

图 2 原始多光谱与全色图像

(a) 第 1 组实验数据的 MS; (b) 第 1 组实验数据的 PAN; (c) 第 2 组实验数据的 PAN; (d) 第 3 组实验数据的 PAN; (e) 第 4 组实验数据的 MS; (f) 第 4 组实验数据的 PAN

拟合公式表示为:

$$\mathrm{LRP}_{(i,j)}=\sum_{k=1}^{4}c_k'\mathrm{LRM}_{k(i,j)},P=\frac{\max(\mathrm{HP})-\mathrm{HP}}{\max(\mathrm{HP})-\min(\mathrm{HP})} \quad (3)$$

通常情况下，能量传递函数(modular transfer function, MTF)能补偿同源同时相不同分辨率的遥感图像上空间细节的差别，然而 MTF 曲线很难取得(Garzelli 等, 2008)。相对于频率域的高通滤波器，空间域高通滤波器具有计算简单、处理速度快的优点。后者中，两种常用的高通滤波器为梯度高通滤波器和拉普拉斯高通滤波器。前者可以提取某一方向灰度突变，而后者能检测所有方向的灰度变化情况。本文方法中需要剔除所有高频信息的影响，选用拉普拉斯高通滤波器，可以最大程度的降低高频信息对 LRP 拟合的影响。此外，多光谱与全色图像的空间分辨率代表了图像获取时进入传感器的地面上一定区域的能量，滤波器的核窗口大小的设置应考虑多光谱与全色图像的空间分辨率之比 r 的影响。本文认为，全色图像中某像元代表的细节信息，应考虑以该像元为中心、$(2r+1)\times(2r+1)$的邻域区域内所有像元，故高通滤波器的核窗口大小也应为$(2r+1)\times(2r+1)$。对于 IKONOS 图像(r=4m/1m=4)，即高通滤波器核窗口大小为 9×9，所以本文选择的拉普拉斯空间域高通滤波器如式(4)所示。

$$\begin{bmatrix} -1 & -1 & -1 & -1 & -1 & -1 & -1 & -1 & -1 \\ -1 & -1 & -1 & -1 & -1 & -1 & -1 & -1 & -1 \\ -1 & -1 & -1 & -1 & -1 & -1 & -1 & -1 & -1 \\ -1 & -1 & -1 & -1 & -1 & -1 & -1 & -1 & -1 \\ -1 & -1 & -1 & -1 & 80 & -1 & -1 & -1 & -1 \\ -1 & -1 & -1 & -1 & -1 & -1 & -1 & -1 & -1 \\ -1 & -1 & -1 & -1 & -1 & -1 & -1 & -1 & -1 \\ -1 & -1 & -1 & -1 & -1 & -1 & -1 & -1 & -1 \\ -1 & -1 & -1 & -1 & -1 & -1 & -1 & -1 & -1 \end{bmatrix} \quad (4)$$

式(3)改写成矩阵形式为:

$$\mathrm{LRP}=C'\times\mathrm{LRM}\quad(\text{权为 }P) \quad (5)$$

$$C'=(\mathrm{LRM}^{\mathrm{T}}\times P\times L\mathrm{RM})^{-1}\mathrm{LRM}^{\mathrm{T}}\times P\times\mathrm{LRP}$$

式中，C'为回归系数；P 为最小二乘求解的权系数，为对角阵，该矩阵能较好的避免因细节边缘像元引入的观测值粗差，提高波段拟合精度；其他参数与式(2)中一致。当输入图像很大时，可以采用随机选点的方式，选取一定数量的点求解回归系数。

3.3 质量评价

Q_4(Alparone 等, 2004)能从亮度、对比度、相关系数 3 个方面表现融合结果与参考图像的整体光谱变形程度，本文将其作为融合质量评价指标，如式(6)。

$$Q_4 = \frac{1}{|\omega|}\sum_{w\in\omega} Q_4(z_1, z_2 \mid w)$$

$$Q_4(z_1, z_2) = \frac{4\left|\sigma_{z_1 z_2}\right| \cdot |\bar{z}_1| \cdot |\bar{z}_2|}{(\sigma_{z_1}^2 + \sigma_{z_2}^2)(|\bar{z}_1|^2 + |\bar{z}_2|^2)} \tag{6}$$

式中，z_1、z_2 分别为融合图像和参考图像各波段灰度值组成的四元组。Q_4 越大，说明融合图像与参考图像越相似，融合质量越好，反之越差。虽然 Q_4 的值与选择的窗口大小 w 有关，但是当采用同一大小的窗口时，使用 Q_4 对不同方法的融合质量的评价结果一致(Alparone 等, 2004)，本文中设定窗口大小为 16 像元。

4 实验与分析

首先对 4 组融合实验数据采用 SRF 的方法拟合 LRP，然后基于线性回归的方法拟合 LRP，最后比较 2 种方法的融合结果。在线性回归拟合方法中，对于第 1、4 组融合输入数据，由于图像较大，所以本文随机选择 2000 个点求解加权系数，对于第 2、3 组融合输入数据，分别采用全部像元、随机选 1000 个点、随机选 2000 个点求解加权系数。图 3 分别为 4 组融合实验数据的 HRP 与 LRP 拟合结果图像，其中 HRP 为融合输入全色图像；LRP_SRF 为基于 SRF

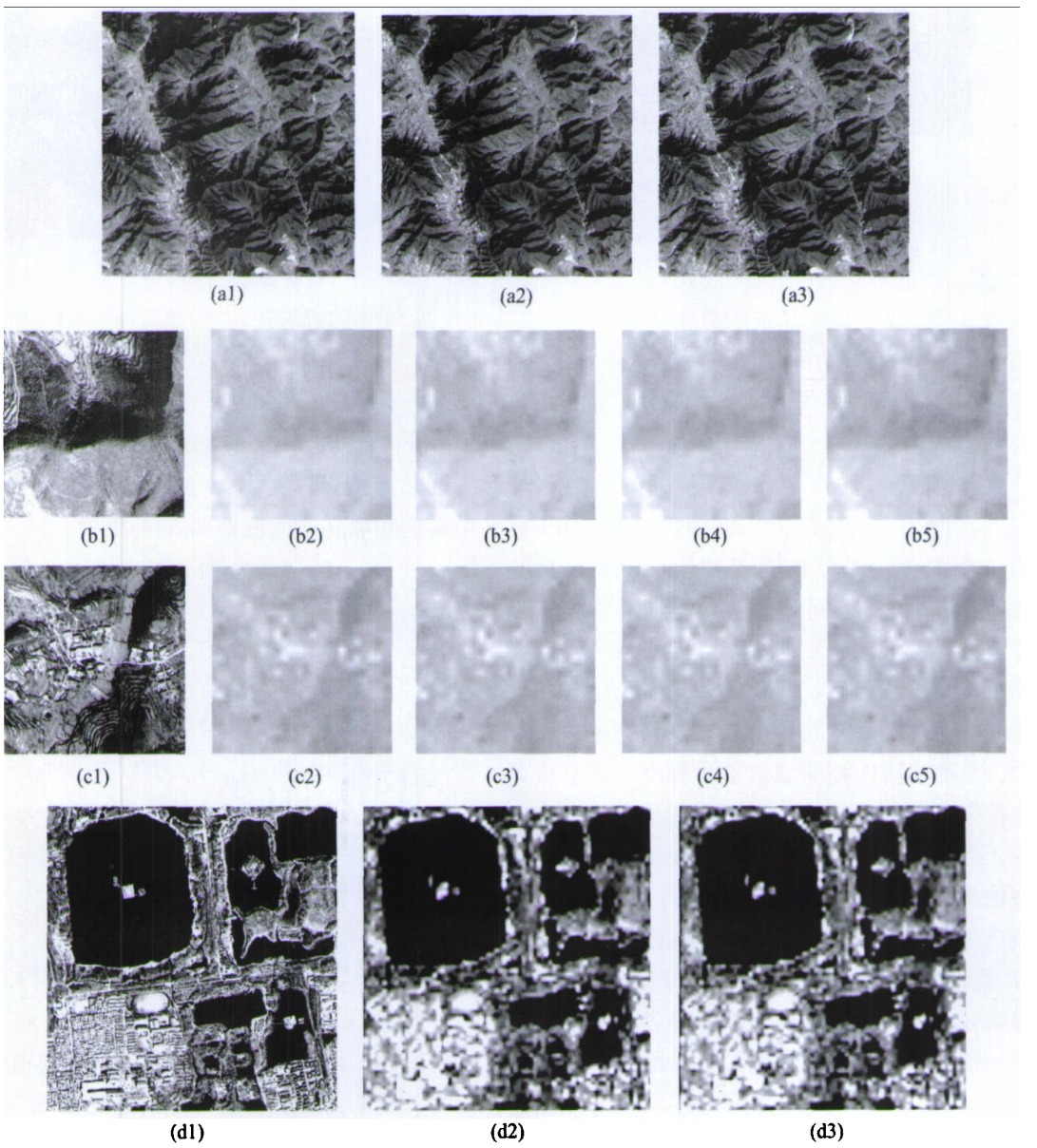

图3 4组融合实验数据的LRP拟合结果

(a1) HRP; (a2) LRP_SRF; (a3) LRP_LS2000; (b1) HRP; (b2) LRP_SRF; (b3) LRP_LSAll; (b4) LRP_LS1000; (b5) LRP_LS2000; (c1) HRP; (c2) LRP_SRF; (c3) LRP_LSAll; (c4) LRP_LS1000; (c5) LRP_LS2000;(d1) HRP; (d2) LRP_SRF; (d3) LRP_LS2000

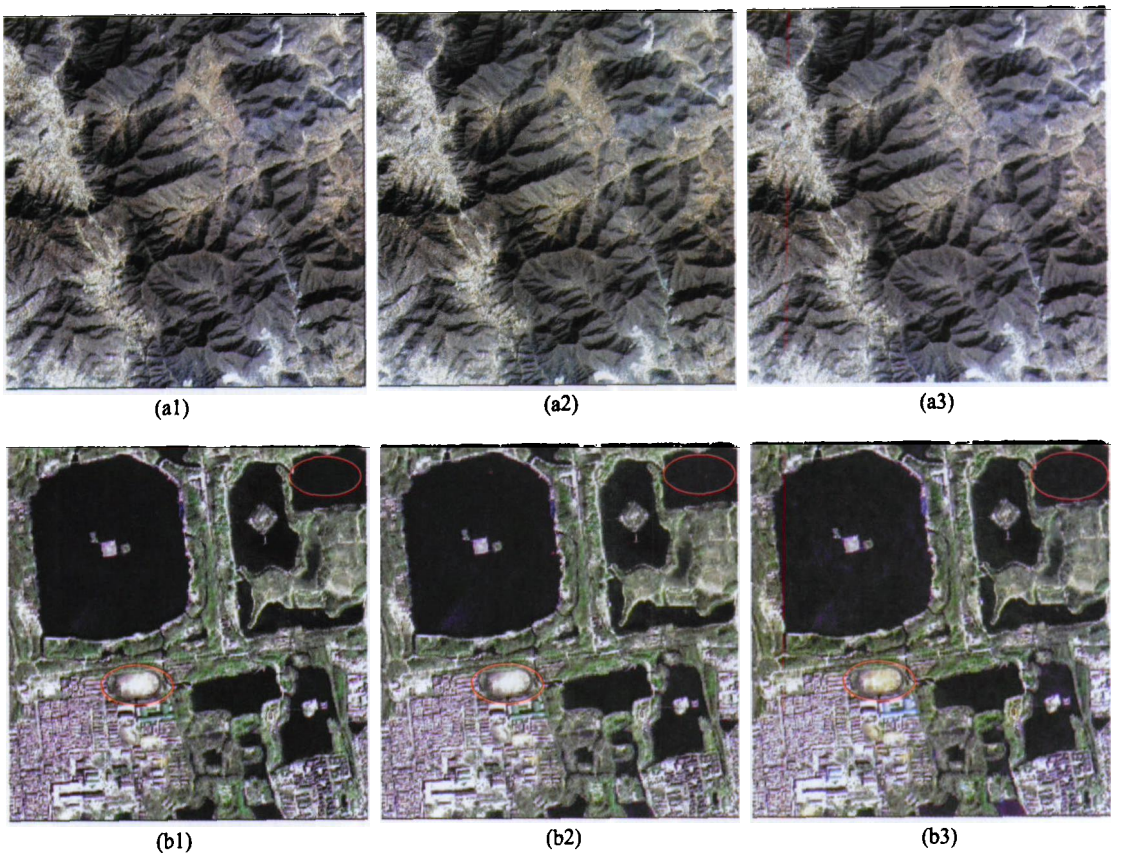

图 4　2 组实验图像基于 LRP_LS2000 和 LRP_SRF 的融合图像

(a1) HRM_FIHS; (a2) HRM _SRF; (a3) HRM_ LS2000; (b1) HRM_FIHS; (b2) HRM _SRF; (b3) HRM_ LS2000

表1　不同方法构造LRP的加权系数与HRP的相关系数，以及Q_4质量评价指标

Dataset	拟合方法	加权系数	与HRP相关系数	Q_4
1	LRP_SRF	0.1965, 0.2350, 0.2367, 0.2454	0.8867	0.8294
	LRP_LS2000	0.1042, 0.1484, 0.3408, 0.3408	0.8872	**0.8303**
	FastIHS	0.2500, 0.2500, 0.2500, 0.2500	0.8866	0.8284
2	LRP_SRF	0.1965, 0.2350, 0.2367, 0.2454	0.8541	0.7921
	LRP_LSAll	0.0241, 0.2817, 0.3236, 0.2882	0.8543	0.7923
	LRP_LS1000	0.0392, 0.2731, 0.2973, 0.3061	0.8543	**0.7926**
	LRP_LS2000	0.0391, 0.2509, 0.3208, 0.3103	0.8543	0.7923
3	LRP_SRF	0.1965, 0.2350, 0.2367, 0.2454	0.6668	**0.8371**
	LRP_LSAll	0.2045, 0.2836, 0.2344, 0.1936	0.6674	0.8366
	LRP_LS1000	0.2909, 0.1200, 0.2906, 0.2290	0.6667	0.8349
	LRP_LS2000	0.2173, 0.3272, 0.0953, 0.2684	0.6665	0.8360
4	LRP_SRF	0.1965, 0.2350, 0.2367, 0.2454	0.7407	0.7987
	LRP_LS2000	0.0500, 0.3695, 0.0500, 0.5095	0.7507	**0.8078**
	FastIHS	0.2500, 0.2500, 0.2500, 0.2500	0.7381	0.7976

的LRP拟合结果图像; LRP_ LSAll、LRP_LS1000、LRP_LS2000分别为采用整幅图像所有像元、随机选择1000个像元、随机选择2000个像元进行线性回归的LRP拟合结果图像。

比较 HRP 和拟合的 LRP, 对于第 1 组融合输入数据, 居民地和道路的亮度值较高, 梯田的亮度值略低, 其次是岩石和山脉, 亮度值最低的是山脉的阴影; 对于第 2 组融合输入数据, 相对而言, 梯田和道路亮度值较高, 岩石次之, 阴影最暗; 对于第 3 组融合输入数据, 按照亮度排序, 依次是居民地、梯田、岩石、阴影; 对于第 4 组融合输入数据, 街区内的道路和房子亮度值很高, 植被次之, 最后是湖泊。综合 4 组融合输入数据的实验结果, 可以看出, 拟合的 LRP 与 HRP 的明暗程度相似, 可以认为基于线性回归的波段拟合方法获得的 LRP 与基于 SRF 的 LRP 拟合结果相近。

FastIHS(Tu, 2004)融合方法采用4个波段的简单平均值作为LRP, 空间细节的注入方式与本文方法

相同，为了说明本文方法的优越性，同样将其作为比较对象。图4为FastIHS融合方法用于第1、4组融合实验数据的结果(HRM_FIHS表示FastIHS的融合结果，HRM_SRF、HRM_LS2000分别表示基于LRP_SRF、LRP_LS2000的融合结果。对于第1组实验数据，所有融合方法得到了高分辨率的多光谱图像，与原始多光谱图像相比，整体颜色极为相近，简单的目视判读很难比较。对于第4组融合实验数据，所有方法同样得到了高分辨率的多光谱图像，但是对于图像右上角的湖泊，HRM_LS2000中的紫色成分更多，与原始多光谱图像更相近，其他2幅融合图像在此区域则相对偏蓝色，对于图像中间区域的运动场，HRM_LS2000方法较好的保留了参考图像中的黄色成分，相对而言，其他2种方法更偏灰或白色，因此，本文方法在保持光谱信息方面具有优越性。由于各融合方法采用的细节注入参数完全一致，所以这种光谱变形主要是构造LRP时的拟合参数引起的。

主观目视比较的差别同样能在定量融合质量评价指标的比较中体现出来。表1为4组融合输入数据采用不同方法构造LRP的加权系数、LRP与HRP的相关系数，以及Q_4融合质量评价指标。

(1) 从LRP与HRP的相关系数，本文方法能有效的拟合出LRP，不同方法的结果相差较小；

(2) 从质量评价指标，基于线性回归波段拟合构造LRP的图像融合方法，能够达到甚至超过基于SRF波段拟合构造LRP的图像融合方法；

(3) LRP_SRF与LRP_LS的加权系数有较大差异，原因在于多光谱图像间存在较大的相关性，使回归方程法方程的设计阵具有一定程度的奇异性，法方程系数阵的条件数很大，导致求解的回归系数(加权系数)不稳定(Wang, 2004)；

(4) 随机选点的方式会对融合质量产生一定影响，但影响不大。

5 结 论

空间细节信息的提取对于全色与多光谱图像的融合至关重要。本文研究了基于线性回归波段拟合的空间细节信息提取方法的可行性。通过4组IKONOS数据的实验，结果表明：基于线性回归波段拟合构造LRP的图像融合质量，能够达到甚至超过基于SRF波段拟合构造LRP的图像融合质量。本文方法不需要SRF作为先验知识，因此具有较高的普适性，值得继续研究。以后的研究方向将主要集中在优化线性回归模型、消除法方程设计阵奇异性以及更多遥感图像的试验等方面。

REFERENCES

Alparone L, Baronti S, Garzelli A and Nencini F. 2004. A global quality measurement of pan-sharpened multispectral imagery. *IEEE Transactions on Geoscience and Remote Sensing Letters*, **1**(4): 313—317

Dou W, Chen Y H, Li X B and Sui D Z. 2007. A general framework for component substitution image fusion: an implementation using the fast image fusion method. *Computers & Geosciences*, **33**: 219—228

Dou W. 2006. Research on the Universal Theoretical Framework for Multi-source Remotely Sensed Data. Beijing: Beijing Normal University

Garzelli A, Nencini F and Capobianco L. 2008. Optimal MMSE pan sharpening of very high resolution multispectral images. *IEEE Transactions on Geoscience and Remote Sensing*, **46**(1): 228—236

María G A, Xavier O, Octavi F and Jesús A M. 2006. A low computational-cost method to fuse IKONOS images using the spectral response function of its sensors. *IEEE Transactions on Geoscience and Remote Sensing*, **44**(6): 1683—1691

Shettigara K V. 1989. A linear transformation technique for spatial enhancement of multispectral images using a higher resolution data set. IGARSS'89, **4**: 2615—2618

Space Imaging. 2008. IKONOS 2 Relative Spectral Response [EB/OL]. http://www.geoeye.com/CorpSite/resource/white papers.aspx. (2 Feb, 2009)

Tu T M, Huang P S, Hung C L and Chang C P. 2004. A fast intensity-hue-saturation fusion technique with spectral adjustment for IKONOS imagery. *IEEE Geoscience and Remote Sensing Letters*, **1**(4): 309—312

Wald L, Ranchln T and Mangolini M. 1997. Fusion of satellite images of different spatial resolutions: assessing the quality of resulting images. *Photogrammetric Engineering & Remote Sensing*, **6**: 691—699

Wang Z J, Ziou D, Armenakis C, Li D R and Li Q Q. 2005. A comparative analysis of image fusion methods. *IEEE Transactions on Geoscience and Remote Sensing*, **43**(6): 1391—1402

Wang Z J. 2004. Determining the ridge parameter in a ridge estimation using L-curve method. *Geomatics and Information Science of Wunan University*, **29**(3): 235—238

Xavier O, María G A, Octavi F and Jorge N. 2005. Introduction of sensor spectral response into image fusion methods: application to wavelet-based methods. *IEEE Transactions on Geoscience and Remote Sensing*, **43**(10): 2376—2385

Zhang Y. 2004. Understanding image fusion. *Photogrammetric Engineering & Remote Sensing*, **6**: 657—661

附中文参考文献

窦闻. 2006. 多元遥感数据像素级融合统一理论框架研究. 北京：北京师范大学资源学院

王振杰. 2004. 用L-曲线法确定岭估计中的岭参数. 武汉大学学报. 信息科学版, **29**(3): 235—238